Infrared Spectra of HCl, DCl, HBr, and DBr in Solid Rare-Gas Matrices*

D. E. MANN AND N. ACQUISTA
National Bureau of Standards, Washington, D. C.
AND
DAVID WHITE
Cryogenic Laboratory, Department of Chemistry, The Ohio State University, Columbus, Ohio

(Received 9 December 1965)

The infrared absorption spectra of HCl, $H^{35}Cl$, DCl, HBr, and DBr isolated in solid rare-gas matrices in the range 4°–20°K are presented. The influence of temperature, dilution, deposition rate variations, as well as the presence of certain impurities, on the spectra are also reported and discussed.

In the fundamental region the spectra normally consist of a few relatively narrow bands or lines which show reproducible and fully reversible variation of intensity and bandwidth with change of temperature. The presence of certain dopants, e.g., N_2, in the halide–noble-gas mixture leads, under suitable deposition conditions, to the replacement of the temperature-dependent features by much narrower temperature-insensitive lines at somewhat shifted frequencies.

The temperature-dependent features have been identified as individual rotation–vibration lines of the matrix-isolated diatomic molecules. Their separations are significantly less than those of the corresponding lines in the free molecule spectra, thereby indicating the existence of hindered molecular rotation in the matrix. The barrier to rotation is interpreted in terms of two different models for the molecule-lattice interactions and their limitations discussed.

The temperature-insensitive lines show no rotational structure, and are normally obtained when N_2 or certain other dopants are present in the gas mixtures from which the matrices are formed at 20°K. They do not appear if the deposition is carried out at 4°K. It is suggested that the rotational quenching may be attributed to the formation of loose couples between halide and N_2 molecules during the condensation process.

INTRODUCTION

THE infrared absorption spectra of HCl in solid argon matrices at 4° and 20°K have been described in our earlier preliminary communications.[1] It was concluded from their highly reproducible location near the center of the gaseous HCl fundamental band, their discrete narrow structure, and their reversible variation of intensity with changes in temperature, that the observed spectral features are consistent with the existence of quantized molecular rotation in the matrix. Lines in the matrix spectra which correlate with the $R(0)$ and $P(1)$ transitions of gaseous HCl were identified, and their reduced separation (when compared with the free molecule transitions) shown to imply a hindrance to free rotation as a consequence of a barrier created by environmental influences. Closer inspection revealed that the $R(1)$ transitions, although expected to occur prominently at 20°K, were just barely detectable and apparently much more highly perturbed than either $R(0)$ or $P(1)$. These preliminary results have served as the basis for recent theoretical investigations,[2,3] in which the effect of lattice-molecule coupling on the rotational motion of the trapped diatomic molecule are examined.

In this paper a more complete description of the earlier work on HCl[1] is presented together with some newer results. The infrared spectra of three other matrix-isolated diatomic halides, DCl, HBr, and DBr, are also presented, in order to provide the basis for further tests of the general applicability of approximations in the two principal models which have been proposed to account for our earlier data.

EXPERIMENTAL

While the general technique of matrix-isolation spectroscopy[4] is by now well established, there are some points of special relevance which are mentioned here. A cryostat of conventional design equipped with sapphire or various salt windows was used. The inner window, on which matrix films were deposited, was mounted between very tightly squeezed indium gaskets in a gold-plated copper housing maintained in good thermal contact with the liquid-helium or hydrogen reservoir. When necessary, temperatures were measured with a calibrated copper–constantan thermocouple attached to the inner window holder. The position of the deposition nozzle, through which the hydrogen halide–rare-gas mixture flowed to the cooled window, was adjusted to give films of maximum uniformity and transparency. Minor changes in the position of the nozzle did not influence the spectra, nor was the composition of the window found to be important. The cooled windows were frequently checked for surface quality and, especially, tightness to ensure the best possible thermal contact.

* This work was supported in part by the Advanced Research Project Agency (Order No. 395, Project Code 3910) and the Office of Naval Research under Contract Nonr-495 (12).

[1] L. J. Schoen, D. E. Mann, C. M. Knobler, and D. White, J. Chem. Phys. **37**, 1146 (1962); Proc. Intern. Symp. Mol. Struct. Spectry., Tokyo, 1962, Lecture A209.

[2] W. H. Flygare, J. Chem. Phys. **39**, 2263 (1963).

[3] H. Friedmann and S. Kimel, J. Chem. Phys. **41**, 2552 (1964).

[4] A. M. Bass and H. P. Broida, *Formation and Trapping of Free Radicals* (Academic Press Inc., New York, 1960).

Mixtures were prepared in accordance with standard manometric techniques. Calibrated Wallace and Tiernan differential gauges were used to ensure precise and reproducible sample preparation. Deposition rates were controlled with Granville–Phillips calibrated leaks, and monitored both by total sample pressure changes registered on a Wallace and Tiernan precision differential manometer and by noting the constancy of the system vacuum on a cold cathode gauge mounted close to the cryostat.

Infrared spectra were taken with a Perkin–Elmer Model 99 double-pass monochromator in which a 300-lines/mm grating was employed as the dispersing element. Suitable filters were used to eliminate all higher-order spectra. Normally a thermocouple detector was used, although on occasion a cooled PbS cell was employed near 2900 cm^{-1}. The actual working resolution was in the range 0.5 to 0.8 cm^{-1} for normal deposits, and 1.0 to 1.5 cm^{-1} for thick deposits and weak lines. Wavelength measurements were made with respect to directly superimposed HCl, HBr, DCl, or DBr gas-phase spectra and are uncertain to approximately $\frac{1}{10}$ the working resolution for the sharp lines.

The HCl, HBr, DCl, and DBr were used as supplied by The Matheson Company Rutherford, New Jersey, and Merck of Canada, Ltd., Montreal. The matrix gases argon, krypton, and xenon were of the highest purity available from The Linde Company.

The $H^{35}Cl$ sample, enriched to approximately 90% ^{35}Cl, was obtained from the Stable Isotopes Division, Oak Ridge National Laboratory. Except for small amounts of $H^{37}Cl$ in $H^{35}Cl$, and HCl in the DCl, and HBr in the DBr no other impurities were detected by infrared analysis.

EXPERIMENTAL RESULTS

It was found, after extensive investigation, that within broad limits changes in deposition rate and dilution had no appreciable influence on the character of the matrix spectra. No significant alteration in the shape, position, or number of the spectral features was noted over the range of dilutions 1:400–1:10 000. For the most dilute mixtures, when thick films were deposited in order to obtain sufficient optical density, decreases in over-all transmission were observed. This necessitated the use of wider slits, which affected only the resolution. It is interesting that the matrix spectra were unaffected in their essential features despite large changes in the deposition rate. It was found convenient and satisfactory to deposit at an average rate of 100–200μM of mixture/min both at 4° and 20°K. Rates up to tenfold smaller and fivefold greater were tried but were found to have no significant influence on the appearance of the main spectral features. This result suggests that the deposition window was in good thermal contact with the refrigerant reservoir, and that for each of the systems studied here the ambient window temperature was the primary factor in determining the efficiency or, perhaps more precisely, the rate of condensation.

The spectroscopic evidence presented in the following sections shows that, in the absence of certain impurities and within the broad limits on dilution and deposition rate given above, the only factor which determines the essential characteristics of a given spectrum is the *temperature* of the matrix. The spectra obtained at 20°K for deposits originally formed at 4°K are identical in all respects with those obtained at 20° for 20°K deposits. A similar independence of the history of the matrix has been observed repeatedly in measurements carried out at 4° and 14°K. Typical spectra of the diatomic molecules in a given rare-gas matrix, formed within the limits already indicated, may therefore be classified solely on the basis of temperature. It has been experimentally verified in this work that the spectra normally obtained for a given system at various temperatures can be *completely*, *reproducibly*, and *repeatedly* interconverted *merely by altering* the temperature of matrix,[5] at least within the limits of present measurements.

The spectrum of HCl (chlorine isotopes in natural abundance) in solid argon is shown in Fig. 1. The matrix was formed at the boiling point of liquid hydrogen (20°K) and cooled to the boiling point of liquid helium (4°K). Reheating to 20°K gave the original spectrum. With the exception of the temperature-independent features, designated "*Q*," this spectrum is identical, in all respects, to the spectrum previously reported.[1] It is characterized, on cooling from 20° to 4°K, by a marked narrowing and intensification of the principal temperature-dependent features at 2888.1 and 2885.9 cm^{-1} and complete disappearance of the relatively weak bands at 2853.6 and 2896 cm^{-1}, the latter being pronounced only in thick films at 20°K. The spectrum of HCl enriched in ^{35}Cl shown in Fig. 2 leaves no doubt that the clearly resolved doublets at 2885.9, 2888.2 cm^{-1} and 2861.5, 2863.6 cm^{-1} in the 4°K spectrum of Fig. 1, are isotopic in origin. The spacings of these isotopic doublets are very close to the doublets of the gas-phase spectrum.

As mentioned earlier, certain impurities were found to have an extremely marked influence on the matrix spectra of HCl. The presence of nitrogen in a concentration comparable with that of the HCl led to almost complete disappearance of the temperature-dependent features and their replacement by a single sharp[6]

[5] Since the thermocouple is mounted on the metal support of the optically transmitting window, the actual temperature of the matrix is not known. Tests have however shown that the temperature difference between the window mount and the body of the window, when indium gaskets are used for thermal contact, is very small. In some experiments to be reported elsewhere in another connection, the reversible dependence of intensity, line position and width, on temperature (for depositions made at 4° or 20°K) was found to extend to at least 30°K for HCl in argon, 40°K for HCl in krypton and 50°K for HCl in xenon.

[6] Measurements made with an instrument having much higher resolving power and to be reported elsewhere show that even at 20°K the linewidths at half-maximum intensity are approximately 0.15 and 0.25 cm^{-1} for HCl in Ar and Kr, respectively.

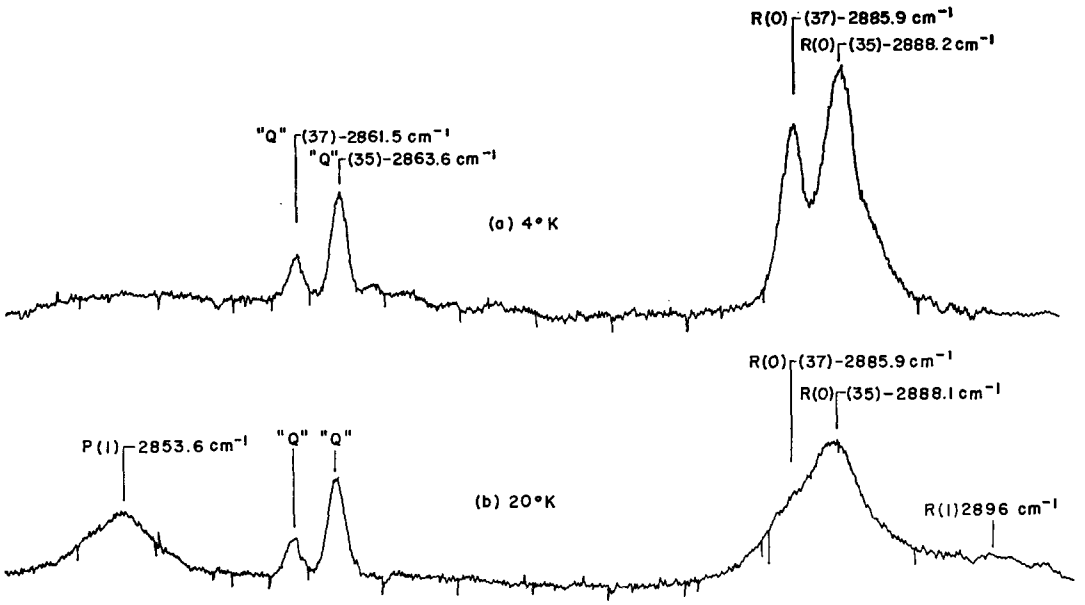

FIG. 1. The infrared spectrum of HCl (chlorine isotopes in natural abundance), trapped in a solid argon matrix at 20°K and cooled to 4°K. Ratio of HCl:argon, 1:1000.

doublet at 2863.6, 2861.5 cm^{-1} that was quite insensitive to temperature variation in the range 4° to 20°K. The presence of residual air or N_2 (less than 0.1%) in the gases used in these experiments or in the vacuum space surrounding the cold window, results in the formation of the "*Q*" feature shown in Figs. 1 and 2. These bands, which were not detected in the earliest experiments,[1] can therefore be avoided by the rigorous exclusion of N_2 or air impurities at all stages of the experiments. The temperature at which the matrix is deposited also influences the relative intensities of the temperature-dependent and temperature-independent features. This is illustrated in Fig. 3. The upper panel of this figure shows a deposition at 20°K for an argon mixture containing trace nitrogen impurity. The "*Q*" of this spectrum feature is quite pronounced. In the lower panel, a spectrum of the same mixture is shown, but where deposition occurred at liquid-helium temperatures. It can be seen that the temperature-insensitive feature, at 2863.6 cm^{-1} found in the 20°K

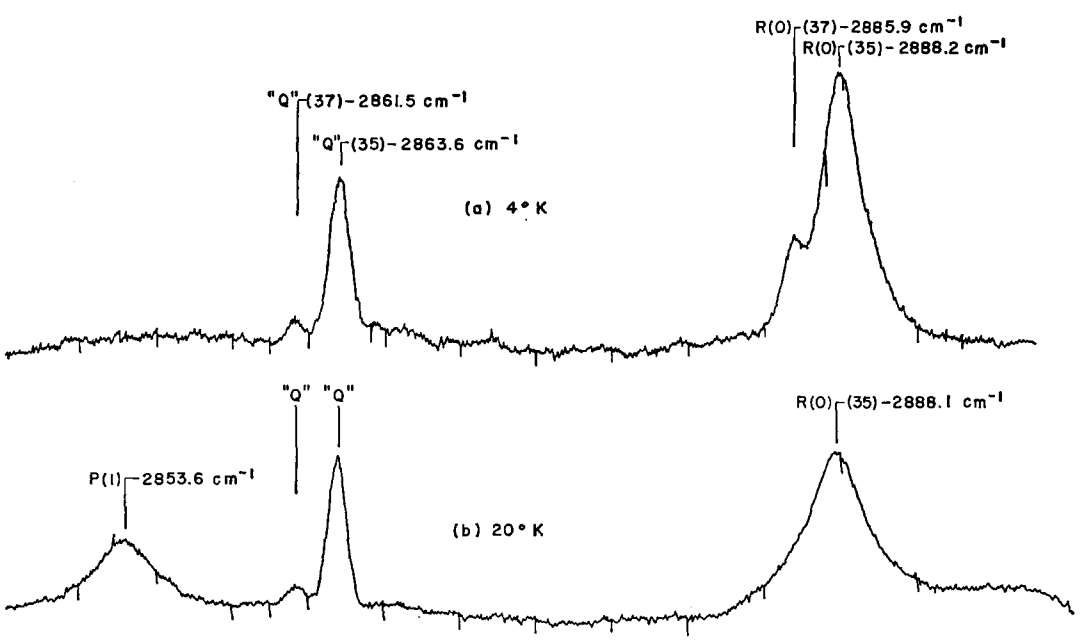

FIG. 2. The infrared spectrum of HCl, enriched in ^{35}Cl isotope, trapped in solid argon at 20°K and cooled to 4°K. Ratio of HCl:argon, 1:1000.

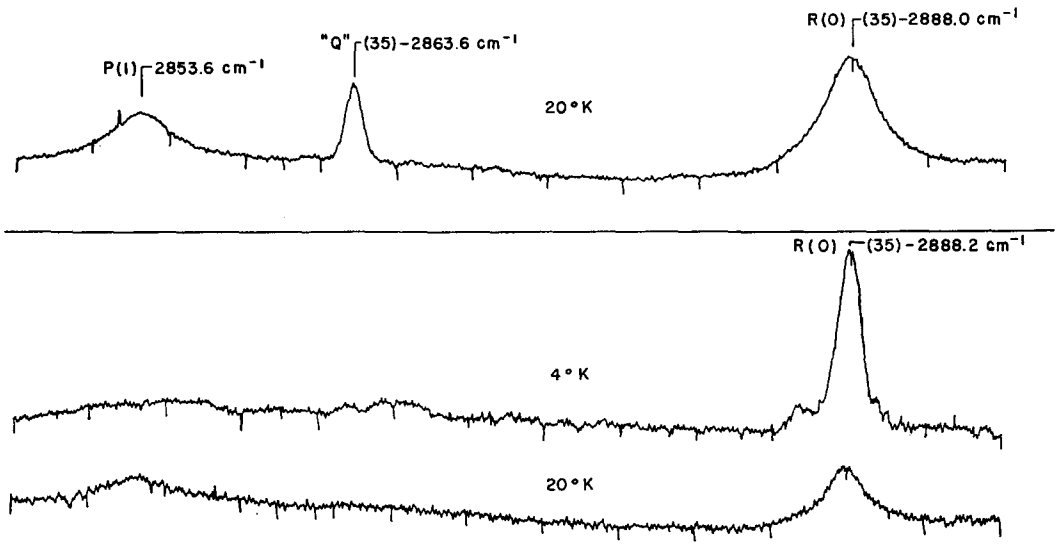

FIG. 3. Upper panel: The infrared spectrum of ^{35}Cl enriched HCl trapped at 20°K in an argon matrix. Lower panel: The infrared spectrum of ^{35}Cl enriched HCl trapped at 4°K in an argon matrix. Ratio of HCl:argon, 1:1000.

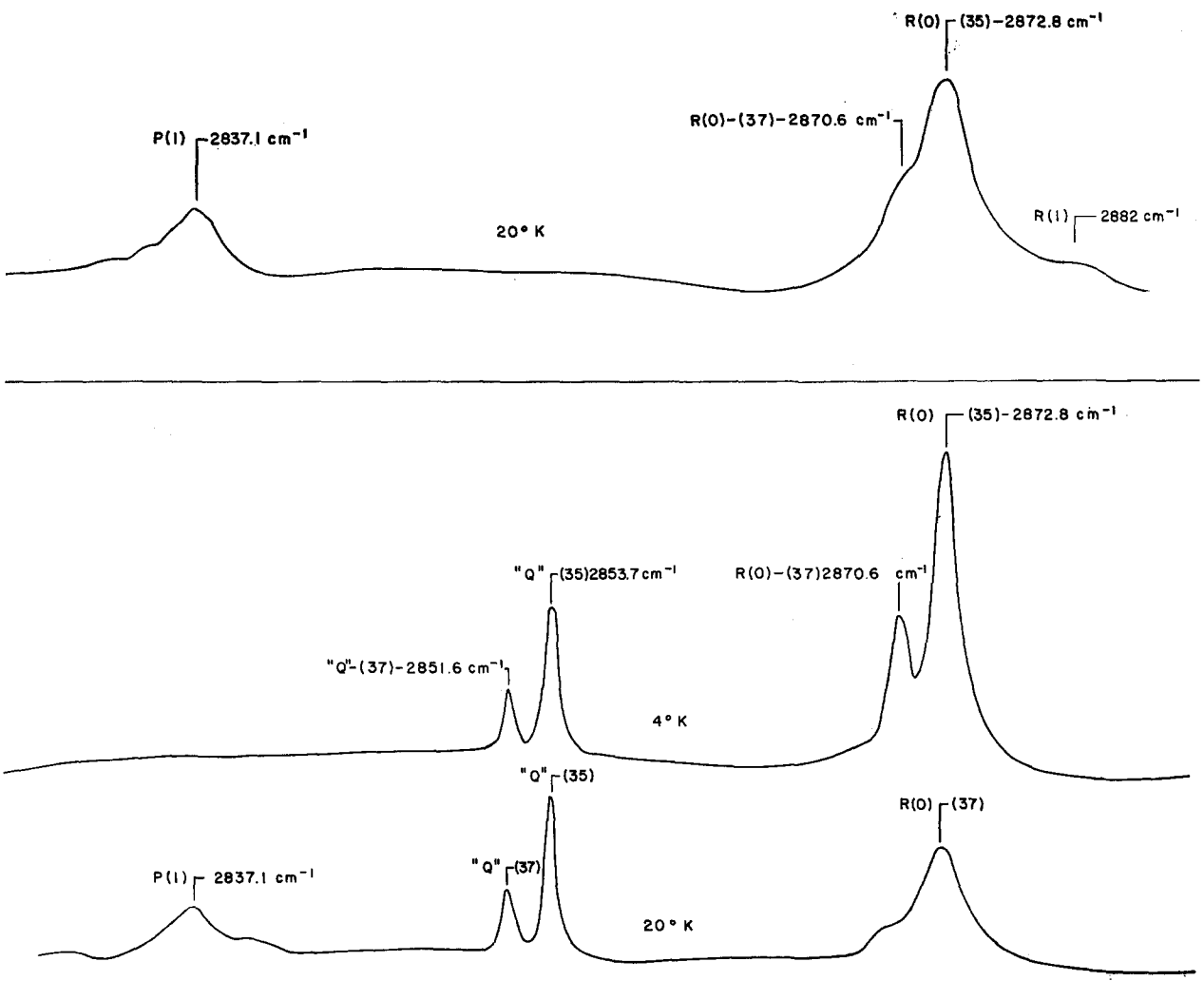

FIG. 4. Upper panel: The infrared spectrum of HCl (chlorine isotopes in natural abundance) trapped at 20°K in a krypton matrix. Ratio of HCl:Kr, 1:1000. Lower panel: Infrared spectrum of DCl trapped at 20°K in a krypton matrix doped with nitrogen and cooled to 4°K. Ratio of HCl:N_2:Kr, 1:1:1000.

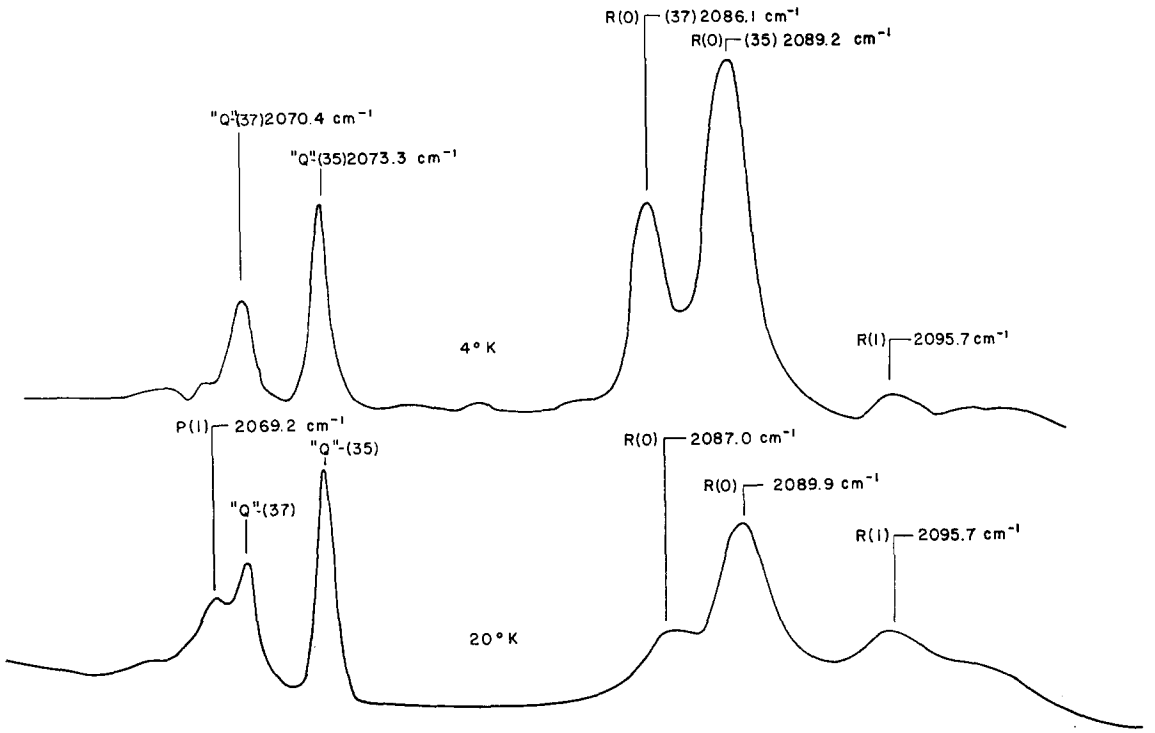

FIG. 5. The infrared spectrum of DCl (chlorine isotopes in natural abundance) trapped at 20°K in an argon matrix and cooled to 4°K. Ratio of DCl:Ar, 1:1000.

deposition experiment, is completely absent from this spectrum, even when the matrix is warmed to 20°K. In general, it is found that lower the temperature of matrix deposition, the lower the intensity of temperature-insensitive bands produced by impurities. Although mention of the significance of this effect is made in the ensuing discussion, a fuller presentation of the data is deferred to a later paper, where the results produced by CO instead of N_2 doping will also be given.

The infrared absorption spectrum of HCl in solid krypton, deposited at the boiling point of liquid hydrogen, is shown in Fig. 4. In this figure as well as all subsequent ones the background noise has been averaged out. The signal-to-noise ratio in these runs was identical to that shown in Figs. 1 through 3. The HCl spectrum in krypton is very similar to the spectrum in the argon matrices. It exhibits both temperature-dependent and temperature-independent features; the former being identified as rotation–vibration lines. The latter, "Q" feature, is much less intense in the krypton matrices than in argon matrices, even with identical nitrogen doping. This result is consistent with the observation that "Q" features are never found in the spectra of even heavily doped mixtures deposited at 4°K, if it is assumed that these lines are due to HCl–N_2 couples formed *during* condensation by a process of surface diffusion or migration. The degree to which the surface migration can be attenuated through the use of lower condensation temperatures, less volatile matrices, or other means would, on the basis of this hypothesis, lead to a corresponding reduction in the intensity of the "Q" lines. It may also be noted that the matrix, once formed, is sufficiently rigid, even in the case of Ar at 20°K, to prevent the formation of "Q" features if they have been avoided initially by deposition at 4°K. Fuller discussion of this and other possible explanations for these observations will be given in a later paper.

The spectra of DCl (chlorine isotopes in natural abundance) trapped in argon and krypton matrices are shown in Figs. 5 and 6. In both cases the deposition was carried out at the boiling point of liquid hydrogen. On temperature cycling from 20°→4°→20°K one finds complete reversibility with respect to band positions, intensities and bandwidths. Like the HCl spectra, the DCl results show both temperature-dependent and temperature-independent features. In Figs. 5 and 6 the frequencies corresponding to the band maxima of the P and R branches of the temperature-dependent features are given. For $R(0)$ and the temperature-independent feature "Q" the frequencies for both the ^{35}Cl and ^{37}Cl isotopes are given. It should be noted that although both sets of traces (Figs. 5 and 6) were obtained under identical deposition conditions, the "Q" feature is much more pronounced in the argon matrix. As in the the HCl matrices, the intensity of the "Q" feature in the DCl spectra is enhanced when the matrix material is doped with nitrogen. The presence of the "Q" bands in the DCl experiments shown in Figs. 5 and 6 where argon and krypton of the highest purity was used, can probably be attributed to residual nitrogen in the

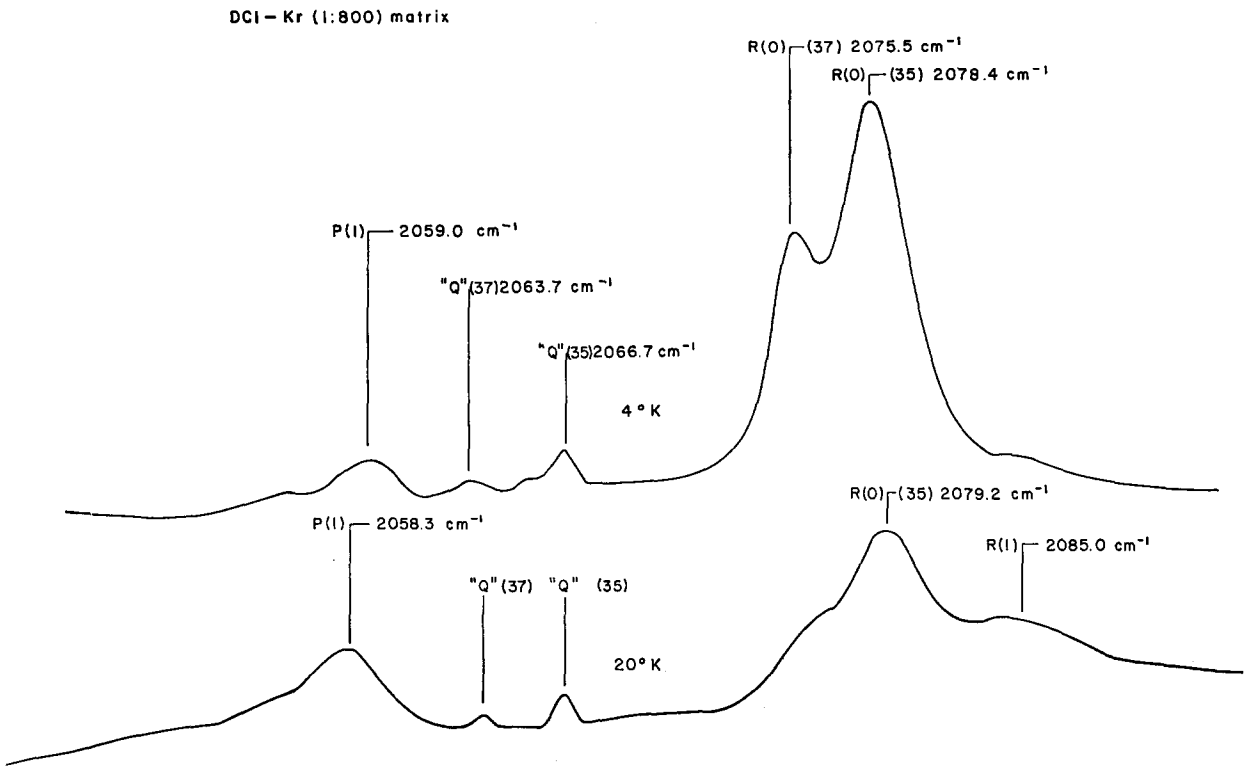

FIG. 6. The infrared spectrum of DCl (chlorine isotopes in natural abundance) trapped at 20°K in a krypton matrix and cooled to 4°K. Ratio of DCl:Kr, 1:800.

vacuum space surrounding the cold window, or degassing from the vessel containing the DCl mixture or the line leading to the Dewar.

A significant difference in the behavior of the two trapped isotopic species, HCl and DCl, apart from the location of the matrix bands relative to the free molecule spectra, is the frequency shift of the rotation–vibration bands [$R(0)$ and $P(1)$], with changes in matrix temperature. The DCl spectra show not only the characteristic line sharpening with decreasing temperature, but also a significant shift in the position of the band maxima. For both the argon and krypton matrices there is a slight shift to the red with decreasing temperature for $R(0)$, whereas for $P(1)$ the shift is to the blue. Thus the rotational spacing, at 20°K, which is already somewhat lower than for the free molecule,[7] is further diminished with decreasing temperature.

The infrared absorption spectrum HBr trapped in a krypton matrix is shown in Fig. 7. The deposition took place at 20°K and temperature cycling showed complete reversibility. In Fig. 7, the spectrum at three different temperatures, the boiling point of hydrogen (20°K) just below the triple point of hydrogen (approximately 13°K) and the boiling point of liquid helium (4°K) are shown. These spectra are very similar to the DCl results, showing both temperature-dependent [labeled $R(0)$, $P(1)$, and $R(1)$] bands and one temperature-independent band ("Q"). As in the DCl case, there is a marked narrowing of the temperature-dependent bands, with decreasing temperature. This is accompanied by a significant shift in frequency of $R(0)$ and $P(1)$ which results in a decrease in the separation between these two bands. This indicates, as in the case of DCl, an increased hindrance to rotation with decreasing temperature.

The HBr spectrum displays some additional features not found in the other hydrogen halide spectra previously described. It can be seen in Fig. 7 that as the matrix is cooled below the temperature at which deposition took place, some new temperature-dependent bands begin to appear on the low-frequency side of $R(0)$. These weak bands appear to grow out of the 20°K base line, increasing in intensity, like $R(0)$, with decreasing temperature. What apparently are very broad lines at 20°K, to the extent that they are practically indistinguishable from background, become sharper lines at lower temperatures. The prominence of $P(1)$ in the middle trace of Fig. 7 is noteworthy. It suggests that the oppositely directed temperature dependence of the population and linewidth factors are relatively in better balance near 13°K than at either higher or lower temperatures for this particular system. The weak but reversible feature which appears at 2545.8 cm^{-1} in the 4°K trace may be an $R(0)$ line arising from

[7] This is discussed in detail in the next section.

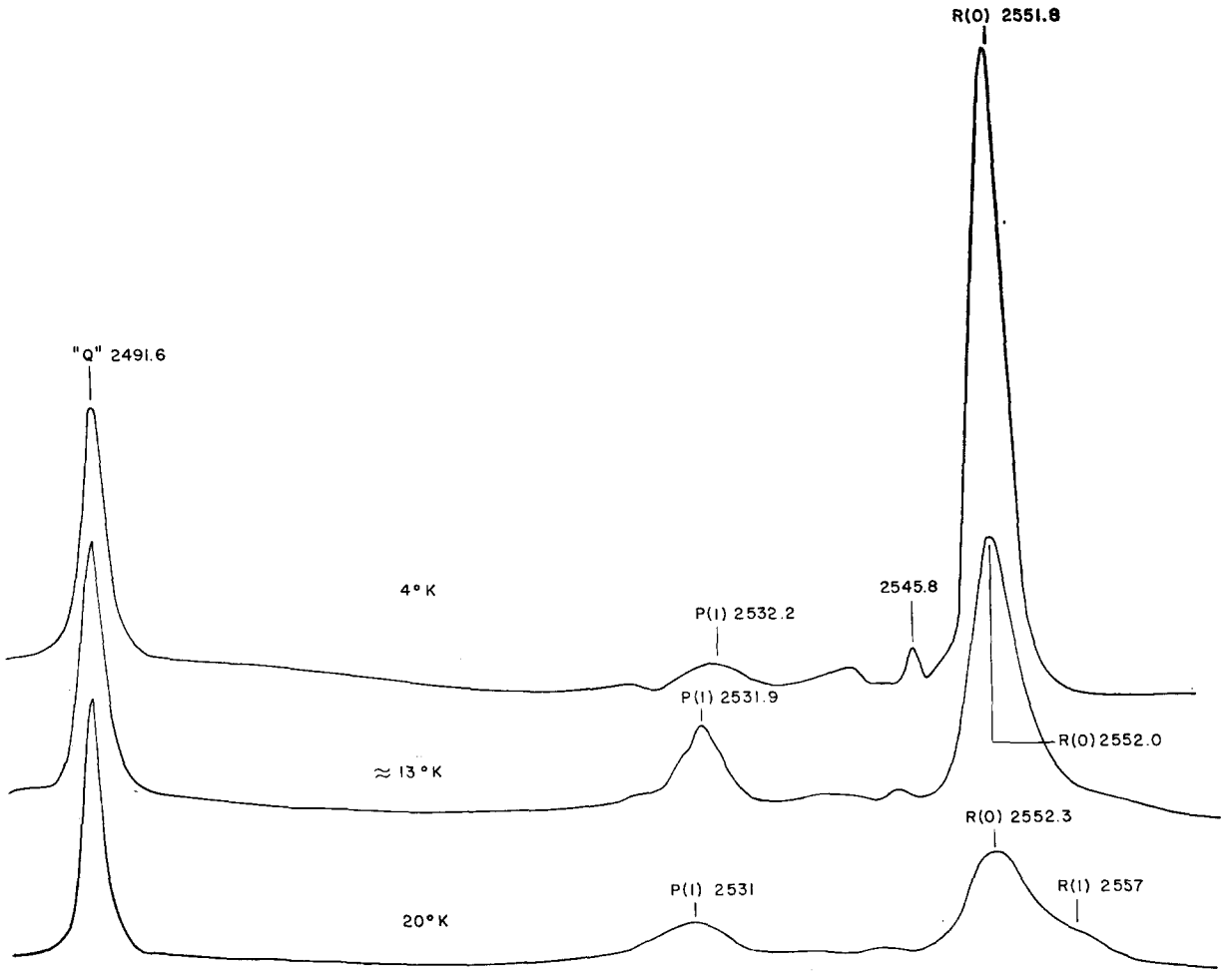

FIG. 7. The infrared spectrum of HBr trapped at 20°K in a krypton matrix and cooled to 13° and 4°K. Ratio of HBr:Kr, 1:500.

HBr molecules trapped at sites somewhat different from those normally occupied by the majority of the isolated halide molecules.

In Fig. 8 the infrared spectra of DBr in a krypton matrix at 4° and 20°K are shown. The deposition took place at the boiling point of liquid hydrogen and like the previous results show complete reversibility on temperature cycling. The DBr spectra are quite different in appearance than the spectra for the other halides. At 20°K there appears a weak but very broad band in the region 1810–1840 cm^{-1} (neglecting the water bands) and a more intense feature at 1790.4 cm^{-1}. It is difficult to distinguish the broad feature from background and for this reason the concentration of DBr in krypton is considerably greater than for the other halides. Careful inspection of the broad feature suggests two overlapping band envelopes, one with a maximum in the vicinity of 1834 cm^{-1} and the other near 1819 cm^{-1}.

On cooling from the boiling point of hydrogen to that of helium there is a marked change in the broad spectral feature in the region 1810–1840 cm^{-1}. From this band envelope (or envelopes) now emerges a series of relatively narrow bands, the most intense occurring at 1833.1 cm^{-1}. This unusual behavior on temperature cycling, characteristic of DBr but not of the other halides previously presented, is possibly associated with its relatively small rotational constant. A somewhat similar effect has been observed for the molecule CO trapped in rare-gas matrices,[8] which has an even smaller rotational constant.

It is difficult, in the case of DBr, to make a one-to-one correlation of the temperature-dependent features with specific rotation–vibration bands of the free molecule. If the change from discrete lines at 4°K to a broad band discrete lines at 4°K to a broad band envelopes at 20°K is a consequence of line broadening rather than overlap of closely spaced higher rotational levels which become populated at higher temperatures, then it is possible to make an assignment of most of the observed bands if it is assumed that the threefold degeneracy of the first excited rotational state $J=1$ of the free molecule is completely lifted in the matrix. Thus the most intense triplet at 4°K 1833.1, 1831.1, and 1826.5 cm^{-1} would

[8] D. E. Mann, N. Acquista, and D. White (unpublished results).

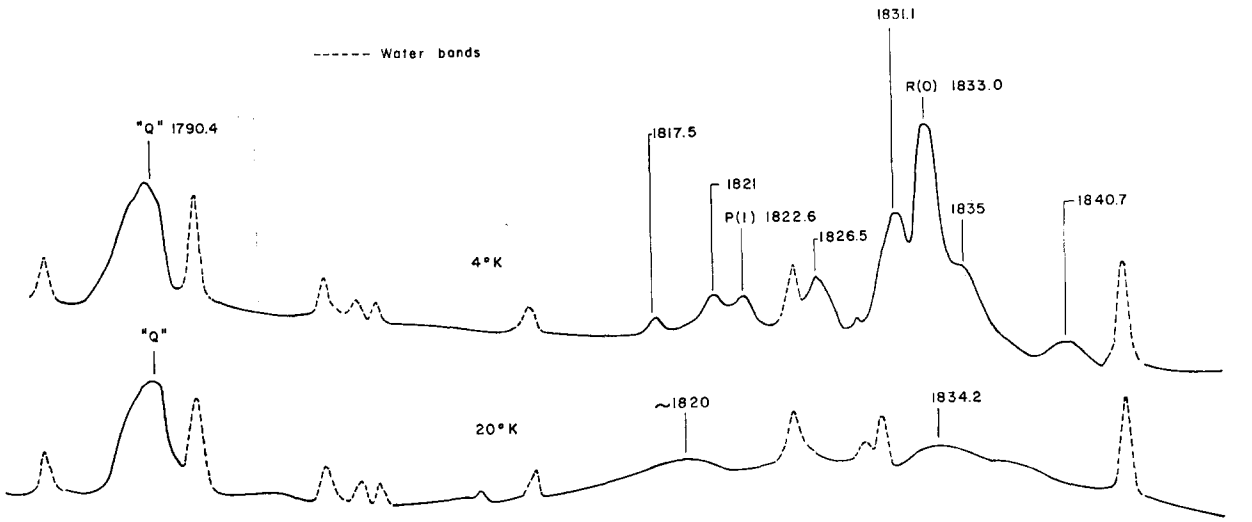

FIG. 8. Solid lines. The infrared spectrum of DBr trapped at 20°K in a krypton matrix and cooled to 4°K. Broken lines, background water spectrum. Ratio of DBr:Kr, 1:400.

correlate with $R(0)$ of the free molecule and the triplet at lower frequencies, 1822.6, 1821.0, and 1817.5 cm^{-1} with $P(1)$. The line separations in each of the triplets are not exactly the same; however, this may in part be due to the difficulty in locating the maxima of the $R(0)$ lines because of overlap by water bands. At 20°K line broadening, which is characteristic of the temperature-dependent features in all the halides investigated, tends to smear out the fine structure thus giving rise to band envelopes, the maximum for $R(0)$ being approximately 1834 cm^{-1} and for $P(1)$ approximately 1820 cm^{-1}. A multiplicity of lines should be expected for $R(1)$, arising from both the splitting of the $J=1$ and $J=2$ rotational states of the free molecule. There are indeed some features to the high-frequency side of $R(0)$ in the 4°K spectrum which can be ascribed to $R(1)$, a shoulder at 1835, 1840.7, and possibly 1844 cm^{-1} overlapping the water band. It is, however, recognized that other hypotheses such as the existence of several slightly different trapping sites, can also account for the multiplets of temperature-dependent features. A distribution of matrix-isolated DBr molecules among three different sites in the krypton lattice would give rise to three pairs of $R(0)$'s and $P(1)$'s each characteristic of a site.

A summary of the experimental data is given in Tables I and II. In Table I, the frequencies of the bands of the bands in the $H^{35}Cl$, $D^{35}Cl$, HBr, and DBr spectra at various temperatures are listed. In Table II, the ^{35}Cl–^{37}Cl isotopic shifts of $R(0)$ and "Q" are given for both HCl and DCl. It can be seen that the observed vibrational isotopic shifts are, within experimental error, identical to those calculated for the free molecule in the rigid-rotator harmonic-oscillator approximation.

TABLE I. Observed frequencies for $H^{35}Cl$ and $D^{35}Cl$ in argon and krypton matrices and HBr and DBr in a krypton matrix.

	Temperature (°K)	$R(0)$ (cm^{-1})	$R(1)$ (cm^{-1})	$P(1)$ (cm^{-1})	"Q" (cm^{-1})
$H^{35}Cl$–Ar	4°	2888.2	···	···	2863.6
	20°	2888.1	2896	2853.6	2863.6
$H^{35}Cl$–Kr	4°	2872.8	···	···	2853.7
	20°	2872.8	2882	2837.1	2853.7
$D^{35}Cl$–Ar	4°	2089.2	2095.7	···	2073.3
	20°	2089.9	2095.7	2069.2	2073.3
$D^{35}Cl$–Kr	4°	2078.4	···	2059.0	2066.7
	20°	2079.2	2085	2058.3	2066.7
HBr–Kr	4°	2551.8	···	2532.2	2491.6
	13°	2552.0	···	2531.9	2491.6
	20°	2552.3	2557	2531.0	2491.9
DBr–Kr	4°	1833.1[a]	···	1826.5[a]	1790.4
	20°	1834	···	1820	1790.4

[a] These represent the highest-frequency temperature-dependent bands in the case of DBr on the assumption that the $R(0)$ and $P(1)$ consist of triplets, see text.

DISCUSSION OF RESULTS

a. Matrix Shifts of Band Centers

In the previous section the observed frequencies for each of the halides were classified according to their

TABLE II. ^{35}Cl–^{37}Cl isotopic shifts of $R(0)$ and "Q" bands of HCl and DCl.

	Temperature (°K)	$R(0)$ $\Delta\nu$ (cm^{-1})	"Q" $\Delta\nu$ (cm^{-1})	Free molecule $\Delta\nu$ (cm^{-1})
HCl–Ar	4°	2.3	2.1	2.1_5
HCl–Kr	4°	2.2	2.1	2.1_5
DCl–Ar	4°	3.1	2.9	3.0_5
DCl–Kr	4°	2.9	3.0	3.0_5

TABLE III. Matrix shifts of vibrational frequencies.

Molecule	Temp (°K)	Gas-phase band center $\nu_g=\frac{1}{2}[R(0)+P(1)]$[a] ($cm^{-1}$)	Matrix band center $\nu_R=\frac{1}{2}[R(0)+P(1)]$[a] ($cm^{-1}$)	$\Delta\nu(1)$ $=\nu_g-\nu_R$ (cm^{-1})	$\frac{\Delta\nu(1)}{\nu_g}$ $\times10^3$	Matrix band center $\nu_Q=$"Q" (cm^{-1})	$\Delta\nu(2)$ $=\nu_g-\nu_Q$ (cm^{-1})	$\frac{\Delta\nu(2)}{\nu_g}$ $\times10^3$
$H^{35}Cl$–Ar	20	2885.7	2870.8	−14.9	5.16	2863.6	−22.1	7.66
$H^{35}Cl$–Kr	20	2885.7	2855.0	−30.7	10.64	2853.7	−32.0	11.09
$D^{35}Cl$–Ar	20	2090.9	2079.6	−11.3	5.40	2073.3	−17.6	8.42
$D^{35}Cl$–Kr	20	2090.9	2068.8	−22.1	10.57	2066.7	−24.2	11.57
$D^{35}Cl$–Kr	4	2090.9	2068.7	−22.2	10.62	2066.7	−24.2	11.57
HBr–Kr	20	2558.5	2541.7	−16.8	6.57	2491.6	−66.9	26.1
HBr–Kr	13	2558.5	2542.0	−16.5	6.45	2491.6	−66.9	26.1
HBr–Kr	4	2558.5	2542.0	−16.5	6.45	2491.9	−66.4	26.0
DBr–Kr	20	1839.7	1827	−12.7	6.90	1790.4	−49.3	26.8
DBr–Kr	4	1839.7	1828.8[b]	−10.9	5.92	1790.4	−49.3	26.8

[a] ν_g is the gas-phase band center calculated from experimentally measured $R(0)$ and $P(1)$. ν_R is the band center for molecules rotating in matrix.

[b] Calculated from highest-frequency components designated $R(0)$ and $P(1)$.

temperature dependence. In all cases two types of bands were found. The temperature-dependent ones were attributed to trapped-halide molecules on lattice sites where a form of hindered rotation is possible. The fact that these rotation–vibration bands are relatively narrow suggests that these lattice sites are nearly identical. A second set of nearly identical sites are responsible for the temperature-independent features, designated as "Q" bands. These presumably are sites in which the rotational motion of the trapped halide is is essentially quenched. A comparison of the vibrational frequencies of the matrix-isolated halides, in the two different sites, with that observed in the gas phase is shown in Table III. In this table the vibrational frequencies for the gas phase[9] and the matrix sites where rotation occurs, represent the centers of the rotation–vibration bands and were taken as midway between $R(0)$ and $P(1)$.

It is evident from Table III that the matrix shifts in the case of the halides are always to lower frequencies, and practically independent of temperature.[10] In general the red shifts are larger for the "Q" features than for the rotating matrix-isolated molecules. This effect is much larger in the case of the bromides than for the chlorides, and is discussed in more detail further in the text. It should be noted that the ratio $\Delta\nu/\nu$, for a given matrix material, is almost the same for the isotopically substituted hydrogen halides. This is in accord the theory of solvent shifts by Buckingham,[11] if it is assumed that the interaction between the trapped-halide molecule and matrix is the same for both the hydrogen and deuterium species.

For the interpretation of the magnitude of the matrix shifts in terms of molecular properties, it is necessary to introduce a model for the interaction of the trapped species with the host lattice. Recently Friedmann and Kimel[12] have made a calculation of such shifts for the hydrogen halides in noble-gas matrices, with a simplified Lennard-Jones and Devonshire cell model[13] to describe the interactions. The calculated[12] and observed frequency shifts are shown in Table IV. The calculated frequency shifts are given in three parts; $\Delta\nu^{dis}$ arising from dispersion forces, $\Delta\nu^{ind}$ arising from induction forces, and $\Delta\nu^{rep}$, the contribution due to repulsion. $\Delta\nu_t$, the sum of the three above contributions to the calculated frequency shift, represents an average over all orientations of the trapped diatomic molecule fixed at a lattice site. Friedmann and Kimel[12] have also considered the frequency shift arising from the motion of the trapped molecule in the cage. This in general is quite small, of the order of 1 cm^{-1}, and positive.

Considering the nature of the approximations in the model[12] and the number of estimated molecular parameters it is remarkable that such good agreement is obtained between theory and experiment for the halide molecules trapped at sites where a form of rotation is possible. [$\Delta\nu(1)=\nu_g-\nu_R$, where ν_g is the band center for the gas phase and ν_R the band center for rotating matrix-isolated molecules, is compared with the calculated $\Delta\nu_t$.] Although the agreement is not quantitative, the theory properly predicts a decrease in frequency shift on going from an argon to a krypton matrix and on substituting HBr for HCl in a given matrix. Like the Buckingham theory this model also predicts that $\Delta\nu/\nu$ is constant for the isotopically substituted halides.

A comparison of the theoretical shifts with the experimental $\Delta\nu(2)$'s [$\Delta\nu(2)=\nu_g-\nu_Q$, where ν_Q is the

[9] *Tables for the Calibration of Infrared Spectrometers. Pure and Applied Chemistry* (Butterworths Scientific Publications, London, 1960), Vol. 1, p. 537.

[10] DBr in a krypton matrix is somewhat ambiguous for $\Delta\nu(1)$, due to the multiplet structure of $R(0)$ and $P(1)$.

[11] A. D. Buckingham, Proc. Roy. Soc. (London) **A248**, 169 (1958).

[12] H. Friedmann and S. Kimel, J. Chem. Phys. "Theory of Shifts of Vibration–Rotation Lines of Diatomic Molecules in Noble-Gas Matrices" (to be published).

[13] J. E. Lennard-Jones and A. F. Devonshire, Proc. Roy. Soc. (London) **A163**, 53 (1937).

TABLE IV. Comparison of experimental with calculated frequency shifts.

Molecule	Calculated frequency shifts[b] $\Delta\nu^{dis}$ (cm^{-1})	$\Delta\nu^{ind}$ (cm^{-1})	$\Delta\nu^{rep}$ (cm^{-1})	$\Delta\nu_t$ (cm^{-1})	Experimental frequency shifts $\Delta\nu(1)=\nu_0-\nu_R$ (cm^{-1})	$\Delta\nu(2)=\nu_0-\nu_Q$ (cm^{-1})
$H^{35}Cl$–Ar	−66.6	−2.5	44.9	−24.2	−14.9	−22.1
$H^{35}Cl$–Kr	−66.7	−2.5	37.9	−31.3	−30.7	−32.0
$D^{35}Cl$–Ar	−47.1	−1.8	31.7	−17.2	−11.3	−17.6
$D^{35}Cl$–Kr	−47.2	−1.9	26.8	−22.3	−22.1	−24.2
HBr–Kr	−57.1	−0.4	48.1	−9.4(−20)[a]	−16.8	−66.9
DBr–Kr	−40.4	−0.3	34.0	−6.7(−14)[a]	−11.8[c]	−49.3

[a] The Lennard-Jones parameters for the two halides HCl and HBr were not derived from the same type of experimental data (see Ref. 12). The parameters for HCl were obtained from second virial coefficients and viscosities whereas those for the bromide from critical constants. In the case of HCl the critical constants give a value for ϵ too small and σ too large. If one increases ϵ(HBr) and increases σ(HBr) by the same ratio as in HCl, the values in the brackets are obtained.

[b] Interactions in this model are expressed in terms of pair interactions given by the Lennard-Jones potential function. The parameters σ and ϵ for this potentional function were assumed to be the same for the isotopic halides.

[c] Experimental frequency shifts are those at 20°K except for DBr which is an average of the 4° and 20°K shifts.

frequency of the matrix-isolated halide trapped at a site where rotation is quenched] shows reasonable agreement for the hydrogen chlorides but very poor agreement for the bromides. In the case of the hydrogen chlorides it was shown that the "Q" bands were related to the presence of trace nitrogen impurity in the rare-gas matrix. If it is assumed that the halide molecules, which give rise to these "Q" bands, are trapped in sites where one or more of its nearest neighbors is a nitrogen molecule, then the total interaction is changed. The magnitude of this interaction, averaged over all orientations of the central halide molecule, should however not differ greatly from the case where all the nearest neighbors are rare-gas atoms. In the Lennard-Jones approximation of the pair interaction, the force constants for N_2–hydrogen halide interactions are nearly the same as Ar–hydrogen halide interactions and somewhat smaller than Kr–hydrogen halide interactions.[13] Thus one would expect $\Delta\nu(1)\gtrsim\Delta\nu(2)$, $\Delta\nu(1)$ being in general greater than $\Delta\nu(2)$ since motion of the trapped diatomic molecule in the cage would, as Friedmann and Kimel[12] have shown, tend to decrease the magnitude of the red shift. It should be noted that although the total interaction between a trapped hydrogen halide and its nearest neighbors may not be altered significantly by substitution of a rare-gas atom by a nitrogen molecule in the cubic lattice, the angular dependence of this interaction could be markedly changed. Thus it is not surprising to find that the rotational motion in sites where the nearest neighbors are all noble-gas atoms (more nearly isotropic case) is considerably less perturbed than in sites influenced by nitrogen molecules. This angular anisotropy may also be a consequence of a change in crystal structure. Barrett and Meyer[14] have recently observed a transformation from face-centered-cubic to hexagonal form on nitrogen doping of rare-gas solids.

The large red shifts of the "Q" bands of the isotopic hydrogen bromides cannot be readily explained if they are a result of hydrogen bromide–nitrogen couples. The fact that $\Delta\nu/\nu$ for the "Q" features (Column 9, Table III) of the two isotopic bromides is constant, is characteristic of a solvent shift. The magnitudes of the shifts cannot, however, be accounted for by the theory of Friedmann and Kimel.[12] An alternative explanation is that these bands are due to matrix-isolated hydrogen bromide pairs. The increase in concentration, which, in the bromide experiments, was necessary to observe the weak broad temperature-dependent bands at 20°K, increases the probability of adjacent halide molecules being trapped in the matrix. Such couples could account for a larger red shift than halide–nitrogen couples. The HCl, DCl experiments do not, however, support this hypothesis. As mentioned earlier, the HCl, DCl spectra were unaffected by concentration changes over the entire range 1:400 to 1:1000. Only one "Q" feature is observed in each of the spectra, attributable to the presence of small amounts of nitrogen or air in the matrix, and its location is independent of the hydrogen chloride concentration.

b. Matrix Shifts of Rotational–Vibration Bands

The spectra of the matrix-isolated halides consist of a number of temperature-dependent bands. With the exception of DBr, a maximum of three such bands are found in the spectrum of each diatomic halide. From the location of these bands and their changes in intensity on temperature cycling they have been identified as rotation–vibration bands which correlate with $R(0)$, $P(1)$, and $R(1)$ of the free molecule. Because of the large rotational constants of these hydrogen halides, it is not surprising, at low temperature, to observe only transitions from the ground and first excited rotational states. A comparison of the separation of the matrix rotational bands with that of the gaseous hydrogen halides is shown in Table V. It is evident from this table that the $R(0)$–$P(1)$ separations in the matrix are smaller than that of the free molecule. This is also true

[14] C. S. Barrett and L. Meyer, J. Chem. Phys. **42**, 107 (1965).

TABLE V. Matrix shifts of rotational lines.

Molecule	Temp (°K)	Matrix $R(0)-P(1)$ (cm^{-1})	Gas $R(0)-P(1)$ (cm^{-1})	Matrix $R(1)-R(0)$ (cm^{-1})	Gas $R(1)-R(0)$ (cm^{-1})	$\frac{[R(0)-P(1)]_{matrix}}{[R(0)-P(1)]_{gas}}$	$\frac{[R(1)-R(0)]_{matrix}}{[R(1)-R(0)]_{gas}}$
HCl–Ar	20	35.5	41.1	8.1	19.7	0.86	0.41
HCl–Kr	20	35.7	41.1	9.2	19.7	0.87	0.47
DCl–Ar	20	20.7	21.3	5.8	10.3	0.97	0.56
	4	<20	21.3	6.5	10.3	<0.94	0.63
DCl–Kr	20	20.9	21.3	5.8	10.3	0.98	0.56
	4	19.4	21.3	•••	10.3	0.91	•••
HBr–Kr	20	21.3	32.9	4.7	15.8	0.65	0.30
	4	19.6	32.9	(−6.0)[a]	15.8	0.60	−0.38
DBr–Kr	20	<14[b]	16.8	•••	8.2	<0.83	•••
	4	6.6	16.8	(1.9)[c]	8.2	0.39	0.23

[a] This value is obtained if it is assumed that $R(1)$ is not the weak shoulder at 2557 cm^{-1} observed as 20°K but the sharp feature at 2545.8 cm^{-1} in the 4°K spectrum.

[b] For DBr at 20°K, only two weak and very broad bands are observed. The highest-frequency band probably overlaps both the $R(0)$ and $R(1)$ features and the value given is probably an upper limit.

[c] This value is obtained assuming the shoulder at 1835 cm^{-1} to the high-frequency side of the most intense $R(0)$ line, is the closest $R(1)$ line.

of $R(1)$–$R(0)$, although it should be pointed out that the location of $R(1)$ is subject to a large uncertainty. The $R(1)$ feature in the matrix appears as either a shoulder on the intense $R(0)$ feature, or, as in the case of DCl, a very broad and weak band. It should also be noted that with exception of HCl there is a measurable change of the band separations with temperature.

In our first communication,[1] where the spectrum of matrix-isolated HCl was presented and discussed briefly, it was pointed out that the decreased separation of $R(0)$ and $P(1)$ and $R(0)$ and $R(1)$, of the matrix spectrum, (relative to the gaseous spectrum) could be accounted for on the basis of a symmetry argument. For purposes of illustration, the perturbations of the rotational levels of the hindered rotator in a field of axial symmetry were considered. A more realistic approach however, is the model of Flygare,[2] where the field symmetry is determined by the crystal lattice. Assuming that a trapped molecule is fixed at a substitutional site of the face-centered-cubic lattice of the rare-gas matrix and is constrained to rotational motions about its center of mass, Flygare[2] showed that the rotational barrier is due primarily to the molecular hexadecapolar charge distribution interacting with the fourth gradient of the electric potential at the molecular center of mass due to the lattice charges, when nonbonded repulsive interactions are neglected. The perturbation of the rotational energy states arise from the anisotropic components of the octahedral field V of the lattice given by,

$$V=-K\{P_4^0(\cos\theta)+\tfrac{1}{168}P_4^4(\cos\theta)\cos 4\phi\} \quad (1)$$

the coupling constant K being proportional to the permanent hexadecapole moment of the diatomic molecule. The fact that the lowest molecular multipole which contributes to the angular anisotropy is the hexadecapole is a consequence of the model employed, and derives in particular from the separation of variables, Eq. (13) of Ref. 2. This permits the calculation of the fourth gradient of the electric potential due to the lattice charges from rotationally independent perturbations.

An alternate approach is to simply develop the potential of interaction of the trapped diatomic molecule with the rare-gas lattice in terms of pair interactions involving only nearest neighbors. With the same assumption as made by Flygare,[2] viz., that the dominant interaction with the host lattice arises from London dispersion forces, the total electrostatic interaction energy of the diatomic molecule, having a permanent dipole, quadrupole, etc., with *one* of the nearest-neighbor's noble-gas atoms may be written as[15]

$$V=\tfrac{1}{2}\alpha(\mu^2/R^6)(3\cos^2\theta_i'+1)+(6\alpha\mu Q/R^7)\cos^3\theta' + (9\alpha Q^2/8R^8)(1-2\cos^2\theta_i'+5\cos^4\theta_i')+\text{higher terms}. \quad (2)$$

R is the distance between the molecular center of mass and a nearest rare-gas atom, μ and Q are the point dipole and quadrupole moments, respectively, of the rotating molecule, α is the polarizability of the rare-gas atom, θ_i' is the angle which defines the orientation of molecular (and dipolar) axis with respect to a position vector from the center-of-mass to a nearest-neighbor lattice atom. The quadrupole moment Q is (2) is that defined as Q_{rot} by Hirschfelder *et al.*[15] The first term represents the molecular dipole-induced dipole interaction, the second gives the dipole-induced dipole interaction with the molecular quadrupole, and the last describes the quadrupole-induced dipole interaction. Upon transforming to lattice coordinates and per-

[15] J. O. Hirschfelder, C. F. Curtiss, and R. B. Bird, *Molecular Theory of Gases and Liquids* (John Wiley & Sons, Inc., New York, 1954).

TABLE VI. Coupling constants K/hcB and Q's calculated from experimental $[R(0)-P(1)]$'s.

Molecule	Temp.	K/hcB	Calculated $R(1)-R(0)$ (cm^{-1})	Experimental $R(1)-R(0)$ (cm^{-1})	Q ($\times 10^{-26}$ esu cm^{-2})
HCl-Ar	20°	15	7.5	8.1	19
HCl-Kr	20°	14	7.5	9.2	20
DCl-Ar	20°	5	7.0	5.8	11
	4°	4	7.5	6.5	10
DCl-Kr	20°	4	7.5	5.8	11
	4°	11	5.0	···	18
HBr-Kr	20°	26	0.4	4.7	27
	4°	28	−2.0	(−6.0)	28
DBr-Kr	20°	18	2.5	···	22
	4°	34	−1.5	1.9	30

forming the appropriate lattice sum over the 12 nearest-neighbor atoms of the face-centered-cubic lattice it is found that the term in R^{-7} vanishes and the total electrostatic interaction energy becomes

$$V=-\{(12\alpha\mu^2/R^6)+(9\alpha Q^2/8R^8)\times[14+10(\sin^4\theta\cos^2\phi-\sin^4\theta\cos^4\phi+\cos^2\theta-\cos^4\theta)]+\cdots+\cdots\}, \quad (3)$$

where θ and ϕ are now the polar and azimuthal angular coordinates of the molecule in the lattice frame. It is evident from (3) that the first term giving rise to an angular dependence is that for the quadrupole-induced dipole interaction.

Equation (3) can be rewritten as

$$V=K\{5\sin^4\cos^2\phi-5\sin^4\theta\cos^4\phi+5\cos^2\theta-5\cos^4\theta-1\}+K' \quad (4)$$

or

$$V=-K\{P_4^0(\cos\theta)+\tfrac{1}{168}P_4^4(\cos\theta)\cos 4\phi\}+K', \quad (5)$$

where $K=-9\alpha Q^2/4R^8$ and the constant

$$K'=-[(12\alpha\mu^2/R^6)+(18\alpha Q^2/R^8)]. \quad (6)$$

Except for the constant K', Eq. (5) like (1) is the Devonshire[16] interaction of a diatomic molecule with an octahedral lattice. Devonshire[16] has computed the magnitude of the perturbations of the rotational states for several values of K/hcB, where $B=h/8\pi^2cI$ is the usual rotational constant in cm^{-1}. With increasing K/B it is found that the separation of the energy levels for the lowest three rotational states decreases. The effect of the rotational barrier for the octahedral field, like the axial one, is to reduce the $R(0)$–$P(1)$ and $R(1)$–$R(0)$ separations, the upper state which correlates with $J=2$ of the free molecule being split.

The values of K/B which best fit the experimental $[R(0)-P(1)]$'s are shown in Table VI, together with the values of the quadrupole moments, computed from K of Eq. (5), using unperturbed atomic polarizabilities[17] α and nearest-neighbor distances of the solid noble gases[18] for R.

A comparison between $[R(1)-R(0)]$'s derived from the coupling constants K/B and the experimental values is shown in Table VI. Considering the experimental uncertainty of assignment and position of $R(1)$, the agreement can be considered fair. The calculated quadrupole moments are shown in the last column of Table VI and are in general considerably larger than the upper limits given by Benedict and Herman[19] $Q(\text{HCl or DCl})\approx 6\times 10^{-26}$ esu cm^{-2}, $Q(\text{HBr, DBr})\approx 8\times 10^{-26}$ esu cm^{-2}, deduced from linewidth data. This is not surprising since any angular anisotropy arising from repulsive forces has been neglected in the potential function. In the preceding section where vibrational shifts were discussed, it was found that such forces are significant, at least in the total interaction.

If the model based on field symmetry has any merit, regardless of whether the rotational barrier arises from hexadecapolar or quadrupolar coupling, one should expect the following relation between the coupling constants for the two isotopic halides:

$$(K/B)_{DX}\approx 2(K/B)_{HX}. \quad (7)$$

This is not what is deduced from the experimental data (Column 3, Table VI). Whereas the theory predicts a larger perturbation of the free molecule rotational levels for the isotopic diatomic with the largest moment of inertia, the *opposite* effect is observed experimentally, except perhaps for the hydrogen bromides at 4°K[20] (see last two columns of Table IV). Furthermore the

[16] A. F. Devonshire, Proc. Roy. Soc. (London) **A153**, 601 (1936).

[17] Landolt-Bornstein, *Zahlenmerte und Functionen*, E. Schmidt, Ed. (Springer-Verlag, Berlin, 1951).

[18] E. R. Dobbs and G. O. Jones, Rept. Progr. Phys. **20**, 560 (1957).

[19] W. S. Benedict and R. Herman, J. Quant. Spectry. Radiative Transfer **3**, 265 (1963).

[20] It also should be pointed out that the $R(0)$ and $P(1)$ triplets observed in the case of DBr at 4°K cannot be explained in terms of splitting of the $J=1$ level in the octahedral field.

magnitude of the perturbation is temperature-dependent, the temperature dependence differing for isotopic species. Thus neither the magnitudes of the rotational perturbations for different isotopic species nor their temperature dependence are accountable in terms of a simple symmetry argument.

In the above model, the effect of matrix temperature is not taken into consideration. It may be that at temperatures in the vicinity of the boiling point of liquid hydrogen, the angular anisotropy of the interaction is smeared out by the lattice vibrations, and it is only at very low temperatures that symmetry effects become dominant. This may also account for the large changes in linewidths which are observed on altering the matrix temperature.

In the preceding discussion it has been assumed that when the center of mass of the trapped diatomic molecule is located at a lattice site of the solid matrix, it is at its equilibrium position. This implies that the interaction with the lattice differs for isotopic diatomics since their centers of mass do not coincide. A better approximation is to assume that there exists a center of interaction[21] located at some point between the two atoms which is identical for all isotopic species, but which does not necessarily coincide with their centers of mass. This type of model has been used to explain differences in vapor pressures between isotopic species in the liquid[21,22] and adsorbed state.[23,24] In the case of matrix-isolated diatomic halides the concept of a center of interaction leads only to a change in rotational constants if the center of interaction of the molecule is fixed at a lattice site. For the crystal-field model discussed above where now the rotations occur about the centers of interaction rather than centers of mass, this would simply imply a larger decrease in rotational constant for the hydrogen halide than for the deuterated halide, when the center of interaction lies closer to the hydrogen atom than either centers of mass. To account for the experimental results, however, it is necessary that $(K/B)_{HX} > (K/B)_{DX}$, i.e., $B_{DX} > B_{HX}$ which is not possible.

Recently Friedmann and Kimel[3,12] have shown that removal of the constraint which forces the rotation about a fixed position leads to much better agreement between theory and experiment. The model adopted by these authors is similar to that of Babloyantz[21] which neglects any effects due to anistropy of the crystal field, but which does allow for coupling between rotation and oscillatory motion, of the molecule as a whole. The matrix is considered as an idealized cage in which the molecule is free to rotate but the translational motion restrained. A spherically symmetrical potential field is assumed, such that for any displacement $\mathbf{r}$, of the center of interaction from its equilibrium position in the cage (the origin of the coordinate system) the potential energy $V=\frac{1}{2}Kr^2$ with the harmonic oscillator approximation where $K=4\pi^2\nu^2M$, M the mass of the molecule, and ν the vibrational frequency in the cage. The Hamiltonian, operator for the rigid rotator can then be written as

$$H=-\frac{h^2}{8\pi^2M}\nabla_G^2-\frac{h^2}{8\pi^2I}\times\left\{\frac{1}{\sin\theta}\frac{\partial}{\partial\theta}\left(\sin\theta\frac{\partial}{\partial\theta}\right)+\frac{1}{\sin^2\theta}\frac{\partial^2}{\partial\phi^2}\right\}+\tfrac{1}{2}Kr^2 \quad (7)$$

the coordinates in the Laplacian being those of the center of mass. It is more convenient to transform the coordinates of $\mathbf{r}$ to center of mass than the coordinates of the Laplacian to center of interaction as Babloyantz[21] and Friedmann[22] have done. If the separation between the center of mass and center of interaction along the bond is represented by the scalar a, then the Hamiltonian in center-of-mass coordinates becomes

$$H=-\frac{h^2}{8\pi^2M}\nabla_G^2+\tfrac{1}{2}KR^2-\frac{h^2}{8\pi^2I}\times\left\{\frac{1}{\sin\theta}\frac{\partial}{\partial\theta}\left(\sin\theta\frac{\partial}{\partial\theta}\right)+\frac{1}{\sin^2\theta}\frac{\partial^2}{\partial\phi^2}\right\}+\tfrac{1}{2}Ka^2+K\mathbf{R}\cdot a\mathbf{1}_\Omega, \quad (8)$$

where $\mathbf{R}$ is the displacement vector of the center of mass from the origin, and $\mathbf{1}_\Omega$ the unit vector along the internuclear axis pointing from the center of mass to the center of interaction. The last term of Expression (8) is the coupling between angular and center-of-mass motions. Writing

$$H=H^0+\mathrm{H}', \quad (9)$$

where H^0 is given by the first four terms of (8) and represents the unperturbed Hamiltonian operator, and

$$H'=\mathbf{R}\cdot a\cdot\mathbf{1}_\Omega K. \quad (10)$$

An approximate solution the Schrödinger equation for the Hamiltonian (9) can be obtained if H' is treated as a perturbation. The unperturbed eigenfunctions and eigenvalues are

$$\psi^0=\psi_R(R)\Theta(\theta,\phi) \quad (11)$$

and

$$E^0_{n,J}=(n+\tfrac{3}{2})h\nu+(h^2/8\pi^2I)(J+1)J+\tfrac{1}{2}Ka^2. \quad (12)$$

To second-order perturbation, the corrections to the zeroth-order energies are in first-order zero, since the matrix elements $\langle\psi_i^0\,|\,H'\,|\,\psi_i^0\rangle$ vanish. In second order for the case $n=0$, the molecule in the ground oscillatory state, a reasonable assumption at low temperatures

$$\frac{E^{(2)}_{0,J}}{hcB}=\frac{A\epsilon^3}{2J+1}\left[\frac{J+1}{\epsilon+2(J+1)}+\frac{J}{\epsilon-2J}\right]=\frac{A\epsilon^4}{[\epsilon+2(J+1)][\epsilon-2J]}, \quad (13)$$

[21] A. Babloyantz, Mol. Phys. **2**, 39 (1959).
[22] H. Friedmann, Advan. Chem. Phys. **4**, 225 (1962).
[23] D. White and E. N. Lassettre, J. Chem. Phys. **32**, 72 (1960).
[24] A. Katorski and D. White, J. Chem. Phys. **40**, 3183 (1964).

TABLE VII. Comparison of theory of Friedmann and Kimel[a] with experiment.

Molecule	Temp (°K)	ϵ[b]	$a\times10^8$ (cm)	Calculated $\Delta[R(1)-R(0)]$ (cm^{-1})	Experimental $\Delta[R(1)-R(0)]$ (cm^{-1})
HCl-Ar	20°	5.13	0.084	12.9	11.6
HCl-Kr	20°	4.13	0.083	99.0	10.5
DCl-Ar	20°	9.58	0.050	0.45	4.5
	4°	9.58	0.073	0.97	3.8
DCl-Kr	20°	7.53	0.041	0.36	4.5
	4°	7.53	0.091	1.92	•••
HBr-Kr	20°	5.75	0.095	18.6	11.1
	4°	5.75	0.102	21.3	(21.8)[c]
DBr-Kr	20°	11.29	0.086	1.9	•••
	4°	11.29	0.16	6.6	(6.3)[c]

[a] Reference 12.
[b] The values of ϵ were obtained from Ref. 12 and were derived from the same molecular constants used for the calculation of the vibrational shifts.
[c] These values are highly uncertain.

where $\epsilon=\nu/B$ and $A=-Ma^2/4I$. The form of (13) differs from that given in Refs. 3 and 12, however the observable quantity, which is the change in energy for a $J\rightarrow J'$ transition,

$$\frac{\Delta E_{J\rightarrow J'}}{hcB} = E^0_{0,J'}+E^{(2)}{}_{0,J'}-(E^0_{0,J}+E^{(2)}{}_{0,J})$$
$$=[J'(J'+1)-J(J+1)]\times\left\{1+\frac{4A\epsilon^4}{[\epsilon+2(J'+1)][\epsilon-2J'][\epsilon-2J][\epsilon+2(J+1)]}\right\} \quad (14)$$

is identical to that of Friedmann and Kimel.[3,12] It should be noted that Eqs. (13) and (14) show *no* J dependence in the numerator of the terms which represent the perturbation of the free molecule energy levels.

For $\epsilon\gg J,\ J'$

$$\Delta E_{J\rightarrow J'}/hcB\approx[J'(J'+1)-J(J+1)][1+4A] \quad (15)$$

which is simply the zeroth-order rotational-energy change for molecules with a reduced rotational constant B', given by

$$B'=B[1-(Ma^2/I)]. \quad (16)$$

For $\epsilon\ll J,\ J'$, the energy change

$$\Delta E_{J\rightarrow J'}/hcB\approx[J'(J'+1)-J(J+1)] \quad (17)$$

is identical to the zeroth-order case. Large deviations from (15) and (17) can only be expected when ϵ approaches in magnitude $2J$ or $2J'$, i.e., when a resonance condition is approached. The validity of a second-order perturbation treatment for a near-resonance condition is, however, questionable.

The separations of $R(0)$–$P(1)$ and $R(1)$–$R(0)$ derived from Eq. (14) are

$$R(0)-P(1)=4hcB\left\{1+\frac{4A\epsilon^4}{\epsilon(\epsilon+4)(\epsilon-2)(\epsilon+2)}\right\} \quad (18)$$

and

$$R(1)-R(0)$$
$$=2hcB\left\{1+\frac{4A\epsilon^4}{\epsilon(\epsilon+4)(\epsilon-2)(\epsilon+2)}\left[\frac{\epsilon^2+2\epsilon+24}{\epsilon^2+2\epsilon-24}\right]\right\}. \quad (19)$$

In Eqs. (18) and (19) it can be seen that there are two unknowns A and ϵ. Since $R(0)$–$P(1)$ and $R(1)$–$R(0)$ have been determined experimentally, these constants can in principle be evaluated. However, we adopt the values of ϵ used by Friedmann and Kimel[12] in the explanation of vibrational shifts (see previous section), and calculate the values of "a" which fit the $R(0)$–$P(1)$ data. These are shown in Table VII together with a comparison of the experimental and calculated

$$\Delta[R(1)-R(0)]$$
$$=[R(1)-R(0)]_{\text{gas}}-[R(1)-R(0)]_{\text{matrix}}.$$

The calculated values of "a" in Table VII appear quite reasonable. The difference, $\Delta a=a_{\text{HX}}-a_{\text{DX}}$ should in this model be given by the relation

$$\Delta a=r_0\{(m_{\text{D}}/m_{\text{DX}})-(m_{\text{H}}/m_{\text{XH}})\}, \quad (20)$$

where r_0 is the equilibrium internuclear separation of the atoms, and m the masses. Equation (20) yields $\Delta a=0.034$ for the hydrogen halides and $\Delta a=0.017$ for the hydrogen bromides. In Table VII it can be seen that in some cases this condition is satisfied while in others it is not. It should also be pointed out that for a given diatomic Molecule "a" should be independent of the matrix. For hydrogen chloride, where data are available, this condition is very nearly satisfied.

The agreement between theory and experiment can, in general, be considered as only fair. This model does have the virtue of at least qualitatively accounting for the observation that the rotational shifts of the deuterated isotopes are larger than for the hydrogen isotopes. This cannot be accounted for on the basis of a field symmetry argument. There is little doubt that a model which takes into consideration the fact that the centers of interaction and centers of mass in isotopic diatomics do not coincide, and the consequent coupling of rotation with center-of-mass motion is indeed a more realistic one. A considerably more sophisticated model, one which includes both symmetry effects and lattice vibrations, together with a more exact solution to the Schrödinger equation, is however necessary to account quantitatively for the observations.

ACKNOWLEDGMENTS

The authors would like to express their thanks to Professor O. Schnepp, Professor M. Gouterman, and Professor J. Gaines for many interesting and helpful discussions, to Dr. S. Kimel and Dr. H. Friedmann for for making their paper available to us prior to publication, and to Miss B. Miley for assistance with some of the experimental work during the early stages of this work.

THE JOURNAL OF CHEMICAL PHYSICS VOLUME 44, NUMBER 9 1 MAY 1966

Microwave Spectrum, Vibration–Rotation Interaction, and Potential Function for the Ring-Puckering Vibration of Trimethylene Sulfide*

DAVID O. HARRIS,† HOWARD W. HARRINGTON,‡ ALAN C. LUNTZ, AND WILLIAM D. GWINN
Department of Chemistry, University of California, Berkeley, California

(Received 18 October 1965)

The microwave spectrum of the ground and first four excited states of the ring-puckering mode of trimethylene sulfide has been observed and assigned. From an analysis of the perturbations to the rotational spectrum arising from the coupling of the internal angular momentum with the over-all rotation of the molecule, the separation between the lowest two vibrational levels was determined to be 8229 Mc/sec. Three mixed vibration–rotation transitions have been observed, and give the more accurate value of 8232.5± 0.4 Mc/sec (0.27461 cm^{-1}) for this separation. From the vibration–rotation interaction and the relative intensities of certain lines, the potential function governing the vibration has been determined to be $7.0207Q^4-87.7581Q^2$ cm^{-1}, where Q is the coordinate describing the vibration. The height of the barrier to the planar configuration is 274.2±2 cm^{-1}. The agreement between the far-infrared spectrum that was calculated using this potential function derived from microwave data, and that which was recently observed by Borgers and Strauss, is very good.

On the basis of a dynamic model for the ring-puckering motion in which the atoms move along curvilinear paths with no bond stretching, the coupling constant between the over-all rotation and the internal angular momentum was calculated. It was found to be 170 Mc/sec compared to the experimental value of 176 Mc/sec. The importance of treating the vibrational dependence of the off-diagonal elements of the inertial tensor as being equivalent to vibrational angular momentum is stressed.

INTRODUCTION

DURING the past several years there has been considerable interest in the nature of the low-frequency ring-puckering motion in four-membered rings.[1–4] The nature of the vibration depends on the potential function governing the mode, which in turn depends on the relative magnitudes of two opposing forces of the molecule. One, the ring strain, tends to make the molecule planar since puckering the ring further decreases the already highly strained ring angles and thus increases the potential energy of the molecule. Opposing the ring strain is the barrier to internal rotation which results in a torsional force about the ring bonds. This force tends to make the ring attain a puckered configuration.

Both of these forces are quite large and the final configuration of the molecule represents a delicate balance between the two. If the torsional force dominates, the potential function will have a double minimum with a barrier to the planar configuration. Extensive work on trimethylene oxide

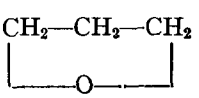

* Presented in part at the Symposium on Molecular Structure and Spectroscopy, The Ohio State University, Columbus, Ohio, 1965 (by D.O.H.) and at The Eighth European Congress on Molecular Spectroscopy, Copenhagen, August 1965 (by W.D.G.).

† Present address: Department of Chemistry, University of California, Santa Barbara, Calif.

‡ Present address: The Hewlett–Packard Company, Palo Alto, Calif.

[1] G. W. Rathjens, N. K. Freeman, W. D. Gwinn, and K. S. Pitzer, J. Am. Chem. Soc. **75**, 5634 (1953).

[2] S. I. Chan, J. Zinn, J. Fernandez, and W. D. Gwinn, J. Chem. Phys. **33**, 1643 (1960).

[3] S. I. Chan, J. Zinn, and W. D. Gwinn, J. Chem. Phys. **34**, 1319 (1961).

[4] S. I. Chan, T. Borgers, J. Russell, H. L. Strauss, and W. D. Gwinn, J. Chem. Phys. **44**, 1103 (1966).